Reduced serum neutralization capacity against SARS-CoV-2 variants in a multiplex ACE2 RBD competition assay

Daniel Junker[1], Alex Dulovic[1], Matthias Becker[1], Teresa R. Wagner[1,2], Philipp D. Kaiser[1], Bjoern Traenkle[1], Ulrich Rothbauer[1,2], Katharina Kienzle[3], Stefanie Bunk[3], Carlotta Strümper[3], Helene Häberle[3], Kristina Schmauder[4,5], Nisar Malek[3,6] ,Karina Althaus[7], Michael Koeppen[8], Michael Bitzer[3,6], Siri Göpel[3,5]*, Nicole Schneiderhan-Marra[1]*

Author Affiliations

[1] NMI Natural and Medical Sciences Institute at the University of Tübingen, Reutlingen, Germany

[2] Pharmaceutical Biotechnology, Eberhard Karls University, Tübingen, Germany

[3] Department Internal Medicine I, Eberhard Karls University, Tübingen, Germany

[4] Institute for medical microbiology and hygiene, University Hospital Tübingen, Germany

[5] German Centre for Infection Research (DZIF), Partner Site Tübingen, Tübingen, Germany

[6] Center for Personalized Medicine, Eberhard-Karls University, Tübingen, Germany

[7] Institute for Clinical and Experimental Transfusion Medicine, University Hospital Tübingen, Tübingen, Germany

[8] Department of Anaesthesiology and Intensive Care Medicine, University Hospital Tübingen, Tübingen, Germany

* Denotes shared senior authorship and corresponding authors.

Contact Information

Nicole Schneiderhan-Marra – Phone number +49 (0)7121 51530 815. Email Address Nicole.schneiderhan@nmi.de Postal Address – Markwiesenstrasse 55, 72770 Reutlingen, Germany.

Siri Göpel – Phone number +49 (0)7071 29 85415. Email Address siri.goepel@med.uni-tuebingen.de Postal Address – Otfried-Müller-Strasse 10, 72076 Tübingen, Germany.

Abstract

As global vaccination campaigns against SARS-CoV-2 proceed, there is emerging interest in the longevity of immune protection, especially with regard to increasingly infectious virus variants. Neutralizing antibodies (Nabs) targeting the receptor binding domain (RBD) of SARS-CoV-2 are promising correlates of protective immunity and have been successfully used for prevention and therapy. To assess neutralizing capacity, we developed a bead-based multiplex ACE2 RBD competition assay as a large scalable, time-, cost-, and material-saving alternative to infectious live-virus neutralization tests. By mimicking the interaction between ACE2 and RBD, this assay detects the presence of Nabs against SARS-CoV2 in serum. Using this multiplex approach allows the simultaneous analysis of Nabs against all SARS-CoV-2 variants of concern and variants of interest in a single well. Following validation, we analyzed 325 serum samples from 186 COVID-19 patients of varying severity. Neutralization capacity was reduced for all variants examined compared to wild-type, especially for those displaying the E484K mutation. The neutralizing immune response itself, while highly individualistic, positively correlates with IgG levels. Neutralization capacity also correlated with disease severity up to WHO grade 7, after which it reduced.

Introduction

Neutralizing antibodies (Nabs) prevent infection of the cell with pathogens or foreign particles by neutralizing them, eliminating a potential threat and rendering the pathogen or particle harmless (1). The longevity of a Nab response has important implications for immune protection and vaccination strategies. In SARS-CoV-2, Nabs interfere with the cell entry mechanism primarily by blocking the interaction of the receptor binding domain (RBD) with the human cell receptor angiotensin converting enzyme 2 (ACE2) (2, 3). The RBD of SARS-CoV-2 is the target of approximately 90 % of the neutralizing activity present in immune sera (4), with a lack of Nabs correlating with risk of fatal outcome (5, 6). Passive transfer of Nabs has been shown to provide protection from infection (7-9), with several Nabs drugs granted emergency use authorization by the U.S. Food and Drug Administration (10-13).

Since the first documented infections in Wuhan China (14), SARS-CoV-2 has continually evolved, with the emergence of global variants of concern (VOC) being of particular importance. As of this moment, the WHO currently lists the alpha (B.1.1.7)(15), beta (B.1.351)(16), gamma (P.1)(17) and delta (B.1.617.2)(18) strains as VOCs (19), in addition to further variants of interest (VOI) such as lambda (C.37)(20). The emergence and disappearance of variants and continual mutation of SARS-CoV-2 is of particular relevance for vaccine development, as all currently licensed vaccines (21-24) only elicit an immune response against the original B1 isolate (hereon referred to as “wild-type”) spike protein (25). Several studies have already found that both convalescent and post-vaccinated sera have lower neutralization capacities against beta and gamma VOCs (26-28). Of particular concern are mutations on amino acid residue (aa) 484 (e.g. E484K), which seem to confer escape from vaccine control, with an additional mutation on aa 501 (e.g. N501Y) increasing this effect (29).

In order to lead development of new vaccines and safely lift social restrictions, definitive correlates of protective immunity are necessary (30). The gold standard for Nabs assessment are virus neutralization tests (VNT), however these require live infectious virions which must be handled in biosafety level 3 (BSL3) laboratories, as well as access to different variants of

74 SARS-CoV-2. In this study we developed and applied a multiplex ACE2 RBD competition
75 assay based upon the antibody-mediated inhibition of RBD-ACE2 binding. This automatable
76 assay enables simultaneous screening of serum samples for the presence of Nabs against an
77 unlimited number of VOCs/VOIs in a single well, making it a time-, material- and cost-effective
78 alternative to live VNTs or classical ELISAs. Following in-depth validation of the assay, we
79 analyzed the IgG antibody response and neutralizing capacity of 325 serum samples from 186
80 COVID-19 patients with mild to severe disease progression towards eleven different SARS-
81 CoV-2 variant RBDs including the alpha, beta, gamma and delta VOCs.

82

Results

ACE2 RBD competition assay validation

To investigate neutralizing capacity of serum from COVID-19 convalescent individuals, we developed and established a high-throughput bead-based multiplex ACE2 RBD competition assay. This assay mimics the ACE2 RBD interaction, detecting the presence of Nabs against SARS-CoV-2. For this, we expressed RBDs of SARS-CoV-2 wild-type and 11 different variants (alpha, beta, gamma, epsilon, eta, theta, kappa, delta, lambda, Cluster 5 and A.23.1) and coupled them on spectrally distinct beads (see methods for details). All beads were then pooled to produce a bead mix, which was incubated with patient serum diluted in assay buffer containing biotinylated ACE2. RBD-bound ACE2 was then detected using phycoerythrin-labeled streptavidin and MFI values were normalized to a control consisting of biotinylated ACE2 without added serum.

Initially, we validated the ACE2 RBD competition assay to standard FDA bioanalytical guidelines. To ensure reagent stability and confirm high assay precision, we measured a sample set of five sera from vaccinated individuals across five independent experiments, identifying that the results of the assay were highly reproducible with minimal variation (as determined by coefficients of variation (%CVs)) (**Figure 1, Supplementary Table 3**). Intra-assay precision was determined using 12 replicates of four samples on a single plate (**Figure 1A**), with %CVs not exceeding 5% for all RBDs (mean range 1.76 - 2.72%). Inter-assay precision (**Figure 1B**) was tested with five samples measured in triplicates in four independent experiments and did not exceed 7 % for any RBD (mean range 2.62 – 4.72%). Short-term temperature stability of the ACE2 buffer was confirmed by incubation for three different durations (2h, 4h, 24h) at two temperatures (4°C and 21 °C) (**Figure 1C**). As a control, freshly prepared buffer was also analyzed. 98 % of %CVs were under 10 % indicating short-term stability of the ready-to-use ACE2 buffer. We examined the stability of the biotinylated human ACE2 stock solution in a freeze-thaw stability experiment (**Figure 1D**), finding no adverse results (all %CVs under 20). Lastly, to investigate the effect of changes in ACE2 concentration

110 on the assay readout, we measured the sample set with a range of ACE2 concentrations (150
111 - 350 ng/mL, **Figure 1E**), with no change in neutralization capacity between different
112 concentrations (mean range 3.54 – 6.49%).

113 To evaluate assay performance against commercially available products, we compared the
114 ACE2 RBD competition assay with the FDA-approved and CE-certified NeutraLISA
115 (Euroimmun) (**Figure 2**). Results between the assays were highly comparable (Pearson's
116 correlation coefficient of 0.7954) (**Figure 2A**). When classifying samples as being either
117 positive or negative, samples with a percentage reduction under 20% are considered negative
118 for the NeutraLISA (31). As both assays detect bound ACE2, we implemented a similar cut-off
119 for the ACE2 RBD competition assay. Overall, 31.7% of samples (59/186) were considered
120 negative in both assays, while a further 54.3% (101/186) were considered positive in both
121 (**Figure 2B)**. Of the remaining samples, six (3.2 %) exceeded 20 % neutralization percentage
122 only in the ACE2 RBD competition assay, while 20 (10.8 %) exceeded 20 % neutralization
123 percentage in the NeutraLISA only.

124 **Neutralization capacities are reduced for all investigated variant RBDs**

125 Following validation, we analyzed neutralization capacities of 325 serum samples from 186
126 COVID-19 patients, including longitudinal samples from 44 donors against RBD wild-type and
127 11 variants (hereafter referred to as "RBD mutants") of SARS-CoV-2.

128 Variant-specific decreases in neutralization capacity compared to wild-type were seen for all
129 RBD mutants (1.1-fold (A.23.1) to 19.7-fold (beta), **Figure 3**). Median neutralization
130 percentage (57 %) was highest in wild-type and lowest (2.9 %) in beta. Among VOC RBD
131 mutants, alpha had the lowest reduction in neutralization capacity (1.25-fold), followed by delta
132 (1.82-fold) and gamma (7.64-fold). Beta had the largest reduction in neutralizing capacity of all
133 variants analyzed (19.71-fold). For the VOIs, lambda had the lowest reduction (3.5 fold),
134 followed by kappa (5.0 fold), eta (6.3 fold) and theta (10.0 fold). The former VOIs Cluster 5
135 (1.3 fold) and epsilon (1.7 fold) had minimal reductions.

136 Neutralization capacity and IgG antibody responses were positively correlated (all Pearsons
137 correlation coefficients above 0.70, **Figure 4**) with variant-specific differences still present. The
138 percentage of samples considered to be negative (<20% neutralization), followed the same
139 variant-specific order as **Figure 3**. For all RBD mutants, the increase in neutralization capacity
140 most commonly occurred once IgG RBD MFI levels exceeded 10,000. Notably, there was
141 individual variation among the samples, with some having high neutralizing capacity but
142 relatively low IgG responses. This was especially true for the RBD wild type and similar
143 performing RBD mutants such as A.23.1, alpha and Cluster 5. For RBD mutants eta, gamma,
144 theta and beta more than 75 % of all samples were considered negative, compared to 42.5 %
145 for wild-type (**Figure 4**).

146 **Neutralization capacity decreases over time**

147 We then examined longitudinal changes on neutralizing capacity and IgG responses using
148 samples from 44 study participants, ranging from 1 to 290 days after the first positive SARS-
149 CoV-2 PCR. For a subset of six individuals with similar sample collection points, both IgG
150 antibody response and neutralization capacity against wild-type (**Figure 5A, B**) remained
151 initially low following infection, with an increase no later than 10 days after the first positive
152 PCR test result, although one individual (Donor3) peaked 6 days after the first positive PCR
153 test and then declined. Neutralization capacity for most individuals (Donors1, 4, 5 and 6)
154 declined no later than 19 days post PCR. Generally, neutralization capacity and IgG levels
155 peaked at similar time points (Donors 1, 2 and 6), although for some individuals (Donors 4 and
156 5) neutralization capacity peaked before IgG titers. Among all longitudinal samples, while
157 neutralization and antibody titers followed a similar pattern (**Figure 5C, D**), responses were
158 highly individualistic with large variances at all time points.

159 As delta represents the current dominant global strain, we then examined how neutralization
160 capacity and antibody binding compared for this variant to wild-type. Neutralizing capacity and
161 IgG binding against delta was reduced for all samples (**Figure 5E and F**). Overall, neutralizing
162 capacity and IgG response followed the same pattern for all samples as for wild-type. When

163 examining all RBD mutants, mean neutralization capacity and IgG antibody responses **(Figure**
164 **5G, H**) clustered as before. Beta, theta and gamma had the largest decrease in neutralizing
165 capacity with eta, kappa and lambda occupying the gap between another cluster of delta,
166 epsilon, Cluster5 and alpha. As expected, all RBD mutants showed reduced neutralization
167 capacity compared to wild-type. Mean neutralization capacity was highly individualistic,
168 peaking for all RBD mutants 22 days post-positive PCR before decreasing below 20 % at
169 approximately 92 days post PCR.

170 **Neutralization correlates with disease severity**

171 We then examined correlations between neutralization capacity and COVID-19 disease
172 severity. Neutralizing capacities for wild-type and RBD delta within 7-49 days post-positive
173 PCR increased steadily with disease severity up to grade 7 (WHO grading scale, hospitalized
174 patients needing intubation and mechanical ventilation), before decreasing for patients of
175 grade 8 (fatal disease course) (**Figure 6A and B)**. Mean neutralization capacities at WHO
176 grade 7 were 72.0 % for wild-type and 58.7 % for delta. From 49 days post positive PCR,
177 neutralization capacities correlated with disease severity (**Figure 6C and D**), however there
178 was an overall reduction for grades 4 to 7 compared to the first timeframe for both wild-type
179 and delta (**Figure 6C and D**). Within this timeframe, mean neutralization capacity for both WT
180 (43.56%) and delta (30.08%) decreased. Anti-RBD IgG levels also correlated with disease
181 severity 7 – 49 days post PCR (**Figure 6E, F**) as well as later than 49 days post PCR (**Figure**
182 **6G, H**) for both wild-type and delta. Peak IgG levels were at grade 7 severity for both wild-type
183 and delta 7 – 49 days post PCR. Post 49 days, mean IgG levels peaked for patients with grade
184 6 severity.

185 **Neutralization correlated with both age and BMI from 49 days post-PCR onwards**

186 Finally, to check for confounding variables, samples taken either 7 to 49 days or more than 49
187 days post-positive PCR were analyzed by their age, gender and BMI (**Supplementary Figure**
188 **1**). Whereas no correlation was observed between neutralization capacity and gender for both
189 timeframes, we found correlations between neutralization capacity and donor age ($p = 0.001$)

190 along with BMI ($p = 0.0179$) for samples drawn more than 49 days after the first positive PCR

191 test (**Supplementary Figure 1D, F**).

192 **Discussion**

193 With vaccination campaigns beginning to take effect and result in reduced case numbers in
194 certain countries, interest in the serological response to SARS-CoV-2 is increasingly changing
195 from quantitative to qualitative in nature. Whereas in the early-phase of the pandemic SARS-
196 CoV-2 antibody assays were helpful in determining seroprevalence and support vaccine
197 development, now a reliable correlate of immune protection is needed to securely lift social
198 restrictions and guide future vaccine developments.

199 While cell-culture based virus neutralization tests (VNTs) (e.g. plaque reduction neutralization
200 test) are the gold standard for neutralization assays, they have many disadvantages over
201 conventional protein-based surrogate assays. Such assays require rapid access to continually
202 changing virus variants and as such special biosafety level 3 laboratories are necessary.
203 Additionally, VNTs are cell-culture based and therefore it takes multiple days to conduct an
204 experiment with reproducibility potentially affected by either the cells or their long culture
205 conditions. Consequently, highly reproducible assays under substantially faster and safer
206 working conditions (e.g. BSL 1) would be highly beneficial. Our newly developed protein-based
207 ACE2 RBD competition assay is finished in under 4 hours and only requires 5 µL of patient
208 sample to measure neutralizing capacities simultaneously against multiple SARS-CoV-2 VOCs
209 and VOIs. As a protein-based assay, it does not require enhanced safety protocols to be
210 followed and can be completed safely in a BSL1 laboratory. Due to the bead-based nature and
211 plate format, it is automatable, suitable for high-throughput, standardized and highly
212 reproducible. The protein-based nature also allows for the rapid inclusion of emerging variants
213 or single mutations.

214 As shown in our technical validation, assay components and as such the results are highly
215 stable. Neutralization percentages correlate with FDA-approved in vitro diagnostic tests such
216 as NeutraLISA (Euroimmun). The lower than 20% reduction cut-off used in the NeutraLISA to
217 identify negative samples is also suitable for the ACE2 RBD competition assay as both
218 measure the steric inhibition of ACE2. Direct comparison between the two assays shows that

219 the ACE2 RBD competition assay has a resolution range more suited to highly neutralizing
220 samples, while the NeutraLISA has increased resolution for samples with weak neutralization
221 at the cost of early saturation of neutralization percentage. Samples which had different
222 classifications between the two assays had a median MFI of 9056, which explains the low
223 neutralization capacities in the ACE2 RBD competition assay, as high neutralization capacities
224 are generally achieved at an MFI > 10,000.

225 Similarly to other authors (32, 33), we identified a significant positive correlation between anti-
226 RBD IgG levels and neutralization capacity. This suggests that neutralizing antibodies
227 represent a consistent portion of all antibodies produced. Overall, our results also show there
228 is a high degree of individualism in responses, with some samples having low titers yet high
229 neutralization capacity for specific RBD mutants. Neutralization itself followed a typical pattern
230 for acute infections with an initial rapid increase which peaks and then declines (34). Notably,
231 neutralizing capacity increased and decreased in parallel to IgG responses, which could have
232 important implications on the immune protection induced by prior infection or vaccination, and
233 should be considered when organizing booster vaccination campaigns. Like other authors (6,
234 35) we identified a correlation between disease severity and neutralizing capacity, however
235 the decrease in IgG levels and neutralizing capacity of patients with WHO disease grade 8
236 (death) has not to our knowledge been reported before. This decrease requires further
237 investigation to determine its cause given its likely role in patient mortality.

238 As expected, neutralizing capacity towards VOCs was highly variable. The strongest
239 reductions in neutralizing capacities were all from variants (eta, gamma, theta and beta) with
240 a E484K mutation. This specific mutation has been reported in multiple studies as an escape
241 mutation that enhances the RBD-ACE2 affinity (36). Neutralizing capacity was further reduced
242 among these variants for those which additionally had a N501Y mutation (gamma, theta and
243 beta), which is known to further enhance RBD-ACE2 binding (37). These results are in-line
244 with previous findings that have reported significant reductions in neutralization for gamma and
245 beta (38-40). The gamma and beta RBDs in our assays are only separated by a single K417N

246 mutation, which is known to significantly reduce both the RBD-ACE2 binding affinity as well as
247 the binding affinity to monoclonal therapeutic antibodies or other human antibodies (41). This
248 reduction in binding affinity could explain why beta neutralizing capacity was lower than
249 gamma. Among recently emerged variants (delta, kappa and lambda), neutralizing capacity
250 compared to wild-type was reduced for all. The reduction in neutralizing capacity seen for
251 kappa and delta are comparable to recent findings (42), although we could not confirm the
252 reduction seen by other authors for Lambda (43). This is likely due to the 7-amino acid deletion
253 in the N-terminal domain of lambda's spike protein, which is not present in the RBD and is
254 thought to contribute to its immune evading properties (44). Overall the decrease in
255 neutralization capacity against RBDs of all analyzed variants compared to wild-type has
256 important implications for the design of second generation vaccines.

257 Our ACE2 RBD competition assay has limitations similar to other protein-based in vitro
258 neutralization assays, such as only accounting for the Nabs that block the RBD-ACE2
259 interaction site through steric hindrance, and not for Nabs that interfere with cell entry
260 mechanisms as would be analyzed in a VNT. Furthermore, the binding assay is also more
261 prone to non-specific binding events. However, a major advantage of the multiplex ACE2 RBD
262 competition assay over VNTs is the speed of response toward viral evolution such as emerging
263 variants of concern. The bead-based format of the assay is also highly reproducible and not
264 susceptible to changes in experimental conditions, as is the case for cell culture based VNTs.
265 The plate format of the assay also enables automation and high-throughput screening. Our
266 ACE2 RBD competition assay only requires recombinant expressed RBD proteins which can
267 be quickly and easily produced. Additionally, this assay has the possibility of introducing
268 artificial mutants to screen for possible escape variants that could arise in the future. Similar
269 to other neutralization studies, our study is limited by the availability of appropriate control
270 samples. Additionally, as the majority of this study population were admitted to the intensive
271 care unit, the more serious grades of COVID-19 infection are heavily overrepresented in our
272 population. Our samples are also highly variable in their longitudinal nature, with no consistent

273 time points. However, this large variation is also beneficial as it clearly demonstrates the
274 individual variability in neutralizing capacity.

275 In conclusion, we have developed and validated an ACE2 RBD competition assay that
276 analyzes neutralizing antibodies in serum for all current variants of concern and interest of
277 SARS-CoV-2. Using this assay, we have identified differing responses in serum from infected
278 individuals, indicating that neutralizing antibody production is directly proportional to total
279 antibody production. Neutralization capacity was highly variable among all variants examined,
280 with the 484 residue appearing to be critical in reducing capacity. Overall, the speed and ease
281 of incorporating new variants into the assay makes it ideal for screening how neutralization
282 capacity changes in emerging variants.

283

284 **Methods**

285 **Sample collection and ethics statement**

286 325 serum samples were collected from 186 patients hospitalized at the University Hospital
287 Tübingen, Germany between April 17, 2020 and May 12, 2021. Longitudinal samples were
288 available from 44 of the 186 patients ranging from 2 to 13 samples per patient. All individuals
289 were tested positive by SARS-CoV-2 PCR. Sample collection and execution of this study was
290 approved by the Ethics committee of the Eberhard Karls University Tübingen and the
291 University Hospital Tübingen under the ethical approval numbers 188/2020A and
292 764/2020BO2 to Prof. Dr. Michael Bitzer. All participants signed the broad consent of the
293 Medical Faculty Tübingen for sample collection.

294 For serum collection, blood was extracted by venipuncture, with the serum blood collection
295 tube rotated 180° two to three times to extract possible air bubbles in the sample. After a
296 minimum coagulation time of 30 minutes at room temperature, serum was extracted by
297 centrifugation for 15 minutes at 2000 x g (RT) and then stored at -80 °C until analysis. Time
298 between blood sampling and centrifugation did not exceed 2 hours.

299 For assay validation, negative pre-pandemic serum samples were purchased from Central
300 BioHub and four previously collected vaccinated samples from healthcare workers vaccinated
301 with the Pfizer BNT-162b2 vaccine (28) were used. The sample collection was approved by
302 the Ethics committee of the Eberhard Karls University Tübingen and the University Hospital
303 Tübingen under the ethical approval number 222/2020BO2 to Dr. Karina Althaus. For all assay
304 validation samples, written informed consent was obtained. Sample characteristics are
305 summarized in **Supplementary Table 2**.

306

307 **Expression and Purification of SARS-CoV-2 RBD mutants**

308 The expression plasmid pCAGGS, encoding the receptor-binding domain (RBD) of SARS-
309 CoV-2 spike protein (amino acids 319-541), was kindly provided by F. Krammer (45).

310 Expression and purification of VOCs alpha, beta and epsilon was carried out as previously
311 described (28). RBDs of SARS-CoV-2 VOCs gamma, delta, eta, theta, kappa and VOI A.23.1
312 were generated by PCR amplification of fragments from wild type or cognate DNA templates
313 and subsequent fusion PCR by overlap extension to introduce described mutations. Based on
314 RBD wild type sequence, primer pairs RBDfor
315 (ATATCTAGAGCCACCATGTTCGTGTTTCTGG), E484Krev
316 (GCAGTTGAAGCCTTTCACGCCGTTACAAGGGGT) and E484Kfor, RBDrev
317 (AAGATCTGCTAGCTCGAGTCGC) for VOC eta and RBDfor, V367Frev
318 (CGGAGTTGTACAGGAAGGAGTAGTCGGCCACGCA) and V367Ffor, RBDrev for VOI
319 A.23.1 were used. VOC lambda was generated based on RBD wild type sequence using
320 primer pairs L452Q-for (GGCAACTACAATTACCAGTACCGGCTGTTCCGGAAG) and
321 L452Q-rev (CGGTACTGGTAATTGTAGTTGCCGCCG), and F490S-for
322 (TCAACTGCTACTCCCCACTGCAGTCCTACGGC) and Lambda-F490S-rev
323 (CTGCAGTGGGGAGTAGCAGTTGAAGCCTTCCAC). VOC delta was generated based on
324 VOC epsilon using primer pairs RBDfor, T478Krev
325 (CGTTACAAGGctTGCTGCCGGCCTGATAGA) and T478Kfor
326 (CCGGCAGCAAGCCTTGTAACGGCGTGGAAG), RBDrev. Based on VOC alpha sequence,
327 VOC theta was generated using primer pairs RBDfor, E484Krev and E484Kfor, RBDrev. VOC
328 kappa was generated based on VOC eta sequence using primer pairs RBDfor, L452Rrev
329 (CGGTACCGGTAATTGTAGTTGCCGCCG) and L452Rfor
330 (GGCAACTACAATTACCGGTACCGGCTGTTCCGGAAG), RBDrev. VOC gamma was
331 generated based on VOC theta sequence using primer pairs RBDfor, K417Trev
332 (GTTGTAGTCGGCGATGGTGCCTGTCTGTCCAGGGG) and K417Tfor
333 (GACAGACAGGCACCATCGCCGACTACAACTACAAG), RBDrev. Amplificates were
334 inserted into the pCDNA3.4 expression vector using XbaI and NotI restriction sites. The
335 integrity of all expression constructs was confirmed by standard sequencing analysis.
336 Confirmed constructs were expressed in Expi293 cells (28, 46). Briefly, cells were cultivated
337 (37 °C, 125 rpm, 8% (v/v) CO_2) to a density of 5.5×10^6 cells/mL, diluted with Expi293F

338 expression medium and transfection of the corresponding plasmids (1 µg/mL) with
339 expifectamine was performed as per the manufacturer's instructions. 20 h post transfection,
340 enhancers were added as per the manufacturer's instructions. Cell suspensions were then
341 cultivated for 2–5 days (37 °C, 125 rpm, 8 % (v/v) CO_2) and then centrifuged (4 °C, 23,900×*g*,
342 20 min) to clarify the supernatant. Supernatants were then filtered with a 0.22-µm membrane
343 (Millipore, Darmstadt, Germany) and supplemented with His-A buffer stock solution (20 mM
344 Na2HPO4, 300 mM NaCl, 20 mM imidazole, pH 7.4). The solution was then applied to a
345 HisTrap FF crude column on an Äkta pure system (GE Healthcare, Freiburg, Germany),
346 extensively washed with His-A buffer, and eluted with an imidazole gradient (50–400 mM).
347 Buffer exchange to PBS and concentration of eluted proteins were carried out using Amicon
348 10K centrifugal filter units (Millipore, Darmstadt, Germany).

349

350 **Bead coupling**

351 The in-house expressed RBD mutants were immobilized on magnetic MagPlex beads
352 (Luminex) using the AMG Activation Kit for Multiplex Microspheres (# A-LMPAKMM-400,
353 Anteo Technologies). In brief, 1 mL of spectrally distinct MagPlex beads (1.25 *10^7 beads)
354 were activated in 1 mL of AnteoBind Activation Reagent for 1 hour at room temperature. The
355 beads were washed twice with 1 mL of Conjugation buffer using a magnetic separator, before
356 being resuspended in 1 mL of antigen solution diluted to 25 µg/mL in Conjugation buffer. After
357 1 h incubation at room temperature the beads were washed twice with 1 mL Conjugation buffer
358 and incubated for 1 h in 0.1 % (w/v) BSA in Conjugation buffer for blocking. Following this, the
359 beads were washed twice with 1 mL storage buffer. Finally, the beads were resuspended in 1
360 mL storage buffer and stored at 4°C until further use.

361

362 **ACE2 RBD competition assay**

363 MULTICOV-AB Assay buffer (1:4 Low Cross Buffer (Candor Bioscience GmbH) in CBS (1x
364 PBS + 1% BSA) + 0.05 % Tween20) was supplemented with biotinylated human ACE2 (Sino
365 Biological, # 10108-H08H-B) to a final concentration of 571.4 ng/mL (ACE2 buffer). Working
366 inside a sterile laminar flow cabinet, serum samples were thawed and diluted 1:25 in assay
367 buffer before being further diluted 1:8 in ACE2 buffer resulting in a final concentration of 500
368 ng/mL ACE2 in all 1:200 diluted samples. Spectrally distinct populations of MagPlex beads
369 (Luminex) coupled with RBD proteins of SARS-CoV-2 wild type and variants alpha, beta,
370 gamma, epsilon, eta, theta, kappa, delta, lambda, Cluster 5 and A.23.1 were pooled in assay
371 buffer (1:4 Low Cross Buffer (Candor Bioscience GmbH) in CBS (1x PBS + 1% BSA) + 0.05%
372 Tween20) to create a 1x bead mix (40 beads/µL per bead population). 25 µL of diluted serum
373 was added to 25 µL of bead mix in each well of a 96-well plate (Corning, #3642). As
374 normalization control, 500 ng/mL ACE2 was used and triplicates of one quality control sample
375 were analyzed on every plate. Samples were incubated for 2h at 21°C while shaking at 750
376 rpm on a thermomixer. Following incubation, the beads were washed three times with 100 µL
377 wash buffer (1x PBS + 0.05 Tween20) using a microplate washer (Biotek 405TS, Biotek
378 Instruments GmbH). For detection of bound biotinylated ACE2, 30 µL of 2 µg/mL RPE-
379 Streptavidin was added to each well and incubated for 45 min at 21 °C while shaking at 750
380 rpm on a thermomixer. Afterwards, the beads were washed again thrice with 100 µL wash
381 buffer. The 96-well plate was placed for 3 min on the thermomixer at 1000 rpm to resuspend
382 the beads before analysis using a FLEXMAP 3D instrument with the following settings: 80 µL
383 (no timeout), 50 events, Gate: 7,500 – 15,000, Reporter Gain: Standard PMT. MFI values of
384 each sample were divided by the mean of the ACE2 normalization control. The normalized
385 values were converted into percent and subtracted from 100 resulting in the percentage of
386 neutralization. Negative neutralization percentages were set to zero.

387

388 **MULTICOV-AB**

389 MULTICOV-AB (46), an in-house produced SARS-CoV-2 antibody assay, was performed with
390 all serum samples to measure RBD-specific IgG levels. The antigen panel was expanded to
391 include RBD proteins from 11 different SARS-CoV-2 variants from which all, except the Cluster
392 5 variant from Sino Biological (# 40592-V08H80), were produced in-house. Briefly, spectrally
393 distinct populations of MagPlex beads (Luminex) coupled with RBD proteins of SARS-CoV-2
394 wild type and variants were pooled in assay buffer (1:4 Low Cross Buffer (Candor Bioscience
395 GmbH) in CBS (1x PBS + 1% BSA) + 0.05% Tween20) to create a bead mix (40 beads/µL per
396 bead population). Samples were diluted 1:200 in assay buffer, working inside a sterile laminar
397 flow cabinet. 25 µL of diluted sample were added to 25 µL of bead mix in a 96-well plate
398 (Corning, #3642) resulting in a total dilution of 1:400. Samples incubated for 2 h at 21°C while
399 shaking at 750 rpm on a thermomixer. After incubation, the beads were washed three times
400 with 100 µL wash buffer (1x PBS + 0.05 % Tween20) using a microplate washer (Biotek 405TS,
401 Biotek Instruments GmbH). Detection of bound antibodies was performed by incubating the
402 beads with 3 µg/mL RPE-huIgG (Dianova, # 109-116-098) for 45 min at 21 °C and 750 rpm on
403 a thermomixer. Following three more washing cycles with 100 µL wash buffer, the beads were
404 resuspended for 3 min at 21°C and 1000 rpm. For readout, a FLEXMAP 3D instrument
405 (Luminex) was used with the following settings: 80 µL (no timeout), 50 events, Gate: 7,500 –
406 15,000, Reporter Gain: Standard PMT.

407

408 **Assay validation**

409 **Intra- and inter-assay precision**

410 To determine the intra-assay precision of the ACE2 RBD competition assay, 12 replicates of
411 four serum samples (Vac1 – Vac4) were measured on a 96-well plate (Corning, #3642).
412 Additionally, 15 replicates of the 500 ng/mL ACE2 control and 12 replicates of a blank control
413 containing only assay buffer without sample or ACE2 were measured. For analysis, the mean,
414 standard deviation and coefficient of variation in percent of all replicates were calculated.

415 For inter-assay precision, four serum samples (Vac1 – Vac4) were measured in triplicates in
416 four independent experiments. Additionally, the quality control, the ACE2 normalization control
417 and blank were also processed in triplicates in the same four experiments. For analysis, the
418 mean, standard deviation and coefficient of variation in percent of all replicates were
419 calculated.

420 **Freeze-thaw stability**

421 Freeze-thaw stability of the biotinylated ACE2 stocks was determined by analyzing five serum
422 samples (Vac1 – Vac4 (vaccinated) and pre-pandemic) in triplicates, with ACE2 stocks
423 undergoing 1 to 6 freeze-thaw cycles. In addition to that, every sample was also processed
424 with ACE2 not re-frozen once thawed (fresh). The MFI values of every sample were normalized
425 to the values of the respective ACE2 control. For analysis, the mean, standard deviation and
426 coefficient of variation in percent of all replicates were calculated.

427 **Short-term stability**

428 Short-term stability was determined by storing ACE2 buffer under six different conditions
429 before proceeding with the assay protocol. The prepared ACE2 buffer was stored 2 h, 4 h and
430 24 h at both 4°C and room temperature and compared to ACE2 buffer without storage (fresh).
431 Replicate MFI values of every sample (Vac1 – Vac4 (vaccinated) and pre-pandemic) were
432 normalized to the values of the respective ACE2 control. For analysis, the mean, standard
433 deviation and coefficient of variation in percent of all replicates were calculated.

434 **Parallelism**

435 To investigate the stability of the ACE2 RBD competition assay against variations of the used
436 ACE2 concentration, five samples (Vac1 – Vac4 (vaccinated) and pre-pandemic) were
437 analyzed with ACE2 concentrations ranging from 150 ng/mL to 350 ng/mL. Replicate MFI
438 values of every sample were normalized to the values of the respective ACE2 control. For
439 analysis, the mean, standard deviation and coefficient of variation in percent of all replicates
440 were calculated.

441 **Commercial assay formats**

442 For further validation, one sample from each individual (n=186) were analyzed with the
443 commercially available in-vitro diagnostic test SARS-CoV-2 NeutraLISA (Euroimmun). The
444 assay was performed according to the manufacturer's instructions. For longitudinal donors with
445 more than one sample available, the sample closest to 20 days after positive PCR diagnosis
446 was picked. Negative neutralization percentages were set to zero.

447 **Data analysis**

448 Data collection and assignment to metadata was performed with Microsoft Excel 2016. Data
449 analysis and visualization was performed with Graphpad Prism (version 9.1.2). Longitudinal
450 curves were fitted using a one-site total binding equation. Correlations were analyzed using
451 Pearson's correlation coefficient. Figures were edited with Inkscape (version 0.92.4). Data
452 generated for this manuscript is available from the authors upon request.

453

454 **References**

455 1. Forthal DN. Functions of Antibodies. *Microbiology spectrum.* 2014;2(4):Aid-0019-
456 2014.
457 2. Jiang S, et al. Neutralizing antibodies for the treatment of COVID-19. *Nature*
458 *biomedical engineering.* 2020;4(12):1134-9.
459 3. Shi R, et al. A human neutralizing antibody targets the receptor-binding site of SARS-
460 CoV-2. *Nature.* 2020;584(7819):120-4.
461 4. Piccoli L, et al. Mapping Neutralizing and Immunodominant Sites on the SARS-CoV-2
462 Spike Receptor-Binding Domain by Structure-Guided High-Resolution Serology. *Cell.*
463 2020;183(4):1024-42.e21.
464 5. Dispinseri S, et al. Neutralizing antibody responses to SARS-CoV-2 in symptomatic
465 COVID-19 is persistent and critical for survival. *Nature communications.*
466 2021;12(1):2670.
467 6. Garcia-Beltran WF, et al. COVID-19-neutralizing antibodies predict disease severity
468 and survival. *Cell.* 2021;184(2):476-88.e11.
469 7. McMahan K, et al. Correlates of protection against SARS-CoV-2 in rhesus macaques.
470 *Nature.* 2021;590(7847):630-4.
471 8. Kim YI, et al. Critical role of neutralizing antibody for SARS-CoV-2 reinfection and
472 transmission. *Emerging microbes & infections.* 2021;10(1):152-60.
473 9. Rogers TF, et al. Isolation of potent SARS-CoV-2 neutralizing antibodies and
474 protection from disease in a small animal model. *Science (New York, NY).*
475 2020;369(6506):956-63.
476 10. Weinreich DM, et al. REGN-COV2, a Neutralizing Antibody Cocktail, in Outpatients
477 with Covid-19. *The New England journal of medicine.* 2021;384(3):238-51.
478 11. (FDA) FaDA. Coronavirus (COVID-19) Update: FDA Authorizes Monoclonal
479 Antibodies for Treatment of COVID-19. https://www.fda.gov/news-events/press-
480 announcements/coronavirus-covid-19-update-fda-authorizes-monoclonal-antibodies-
481 treatment-covid-19. Accessed 23.07.2021.
482 12. Gottlieb RL, et al. Effect of Bamlanivimab as Monotherapy or in Combination With
483 Etesevimab on Viral Load in Patients With Mild to Moderate COVID-19: A
484 Randomized Clinical Trial. *Jama.* 2021;325(7):632-44.
485 13. (FDA) FaDA. Coronavirus (COVID-19) Update: FDA Authorizes Monoclonal
486 Antibodies for Treatment of COVID-19. https://www.fda.gov/news-events/press-
487 announcements/coronavirus-covid-19-update-fda-authorizes-monoclonal-antibodies-
488 treatment-covid-19-0. Accessed 23.07.2021.
489 14. Zhou P, et al. A pneumonia outbreak associated with a new coronavirus of probable
490 bat origin. *Nature.* 2020:1-4.

491 15. Graham MS, et al. Changes in symptomatology, reinfection, and transmissibility
492 associated with the SARS-CoV-2 variant B.1.1.7: an ecological study. *The Lancet*
493 *Public health.* 2021;6(5):e335-e45.
494 16. Tegally H, et al. Detection of a SARS-CoV-2 variant of concern in South Africa.
495 *Nature.* 2021;592(7854):438-43.
496 17. Sabino EC, et al. Resurgence of COVID-19 in Manaus, Brazil, despite high
497 seroprevalence. *Lancet (London, England).* 2021;397(10273):452-5.
498 18. Control ECfDPa. Threat Assessment Brief: Emergence of SARS-CoV-2 B.1.617
499 variants in India and situation in the EU/EEA.
500 https://www.ecdc.europa.eu/en/publications-data/threat-assessment-emergence-sars-
501 cov-2-b1617-variants.
502 19. (WHO) WHO. Tracking SARS-CoV-2 variants.
503 https://www.who.int/en/activities/tracking-SARS-CoV-2-variants/. Updated 06.07.2021
504 Accessed 11.07.2021.
505 20. O'Toole A, and Hill V. Lineage C.37. https://cov-
506 lineages.org/lineage.html?lineage=C.37.
507 21. Skowronski DM, and De Serres G. Safety and Efficacy of the BNT162b2 mRNA
508 Covid-19 Vaccine. *The New England journal of medicine.* 2021;384(16):1576-7.
509 22. Baden LR, et al. Efficacy and Safety of the mRNA-1273 SARS-CoV-2 Vaccine. *The*
510 *New England journal of medicine.* 2021;384(5):403-16.
511 23. Voysey M, et al. Safety and efficacy of the ChAdOx1 nCoV-19 vaccine (AZD1222)
512 against SARS-CoV-2: an interim analysis of four randomised controlled trials in Brazil,
513 South Africa, and the UK. *Lancet (London, England).* 2021;397(10269):99-111.
514 24. Sadoff J, et al. Safety and Efficacy of Single-Dose Ad26.COV2.S Vaccine against
515 Covid-19. *The New England journal of medicine.* 2021;384(23):2187-201.
516 25. Krammer F. SARS-CoV-2 vaccines in development. *Nature.* 2020;586(7830):516-27.
517 26. Jalkanen P, et al. COVID-19 mRNA vaccine induced antibody responses against
518 three SARS-CoV-2 variants. *Nature communications.* 2021;12(1):3991.
519 27. Shen X, et al. Neutralization of SARS-CoV-2 Variants B.1.429 and B.1.351. *The New*
520 *England journal of medicine.* 2021;384(24):2352-4.
521 28. Becker M, et al. Immune response to SARS-CoV-2 variants of concern in vaccinated
522 individuals. *Nature communications.* 2021;12(1):3109.
523 29. Hoffmann M, et al. SARS-CoV-2 variants B.1.351 and P.1 escape from neutralizing
524 antibodies. *Cell.* 2021;184(9):2384-93.e12.
525 30. Krammer F. A correlate of protection for SARS-CoV-2 vaccines is urgently needed.
526 *Nature medicine.* 2021.

527 31. Euroimmun. SARS-CoV-2 NeutraLISA: Produkt-Datenblatt. https://www.coronavirus-
528 diagnostik.de/documents/Indications/Infections/Coronavirus/EI_2606_D_DE_F.pdf.
529 Accessed 19.08.2021.
530 32. Mendrone-Junior A, et al. Correlation between SARS-COV-2 antibody screening by
531 immunoassay and neutralizing antibody testing. *Transfusion.* 2021;61(4):1181-90.
532 33. Grenache DG, et al. Correlation of SARS-CoV-2 Neutralizing Antibodies to an
533 Automated Chemiluminescent Serological Immunoassay. *The journal of applied*
534 *laboratory medicine.* 2021;6(2):491-5.
535 34. Seow J, et al. Longitudinal observation and decline of neutralizing antibody
536 responses in the three months following SARS-CoV-2 infection in humans. *Nature*
537 *microbiology.* 2020;5(12):1598-607.
538 35. Legros V, et al. A longitudinal study of SARS-CoV-2-infected patients reveals a high
539 correlation between neutralizing antibodies and COVID-19 severity. *Cellular &*
540 *molecular immunology.* 2021;18(2):318-27.
541 36. Nelson G, et al. Molecular dynamic simulation reveals E484K mutation enhances
542 spike RBD-ACE2 affinity and the combination of E484K, K417N and N501Y
543 mutations (501Y.V2 variant) induces conformational change greater than N501Y
544 mutant alone, potentially resulting in an escape mutant. *bioRxiv.*
545 2021:2021.01.13.426558.
546 37. Luan B, et al. Enhanced binding of the N501Y-mutated SARS-CoV-2 spike protein to
547 the human ACE2 receptor: insights from molecular dynamics simulations. *FEBS*
548 *letters.* 2021;595(10):1454-61.
549 38. Shen X, et al. SARS-CoV-2 variant B.1.1.7 is susceptible to neutralizing antibodies
550 elicited by ancestral spike vaccines. *Cell host & microbe.* 2021;29(4):529-39.e3.
551 39. Wall EC, et al. Neutralising antibody activity against SARS-CoV-2 VOCs B.1.617.2
552 and B.1.351 by BNT162b2 vaccination. *Lancet (London, England).*
553 2021;397(10292):2331-3.
554 40. Wang P, et al. Antibody resistance of SARS-CoV-2 variants B.1.351 and B.1.1.7.
555 *Nature.* 2021;593(7857):130-5.
556 41. Luan B, and Huynh T. Insights into SARS-CoV-2's Mutations for Evading Human
557 Antibodies: Sacrifice and Survival. *Journal of medicinal chemistry.* 2021.
558 42. Edara VV, et al. Infection and Vaccine-Induced Neutralizing-Antibody Responses to
559 the SARS-CoV-2 B.1.617 Variants. *The New England journal of medicine.*
560 2021;385(7):664-6.
561 43. Kimura I, et al. SARS-CoV-2 Lambda variant exhibits higher infectivity and immune
562 resistance. *bioRxiv.* 2021:2021.07.28.454085.

563 44. Acevedo ML, et al. Infectivity and immune escape of the new SARS-CoV-2 variant of
564 interest Lambda. *medRxiv.* 2021:2021.06.28.21259673.
565 45. Amanat F, et al. A serological assay to detect SARS-CoV-2 seroconversion in
566 humans. *Nature medicine.* 2020;26(7):1033-6.
567 46. Becker M, et al. Exploring beyond clinical routine SARS-CoV-2 serology using
568 MultiCoV-Ab to evaluate endemic coronavirus cross-reactivity. *Nature*
569 *communications.* 2021;12(1):1152.

570

571 **Competing interests**

572 NSM was a speaker at Luminex user meetings in the past. The Natural and Medical
573 Sciences Institute at the University of Tübingen is involved in applied research projects as a
574 fee for services with the Luminex Corporation. The other authors declare no competing
575 interest.

576

577 **Funding**

578 This work was financially supported by the State Ministry of Baden-Württemberg for
579 Economic Affairs, Labour and Housing Construction (grant number FKZ 3-4332.62-NMI-68).

580

581 **Acknowledgements**

582 We thank Johanna Griesbaum, Jennifer Jüngling and Christine Geisler for excellent technical
583 assistance.

584

585 **Author Contributions**

586 DJ and AD conceived the study and designed the experiments. NSM supervised the study.
587 DJ and MaB performed the experiments. DJ, AD, MaB produced components for the
588 multiplex ACE2 RBD competition assay. KK, SB, CS, HH, KS, NM, KA, MK, MB and SG

589 collected samples or organized their collection and provided clinical metadata. PDK, BT, TW
590 and UR produced and designed recombinant assay proteins. MB, SG and NSM procured
591 funding. DJ performed data analysis and generated the figures. DJ and AD wrote the
592 manuscript. All authors critically reviewed and approved the final manuscript.

Figures

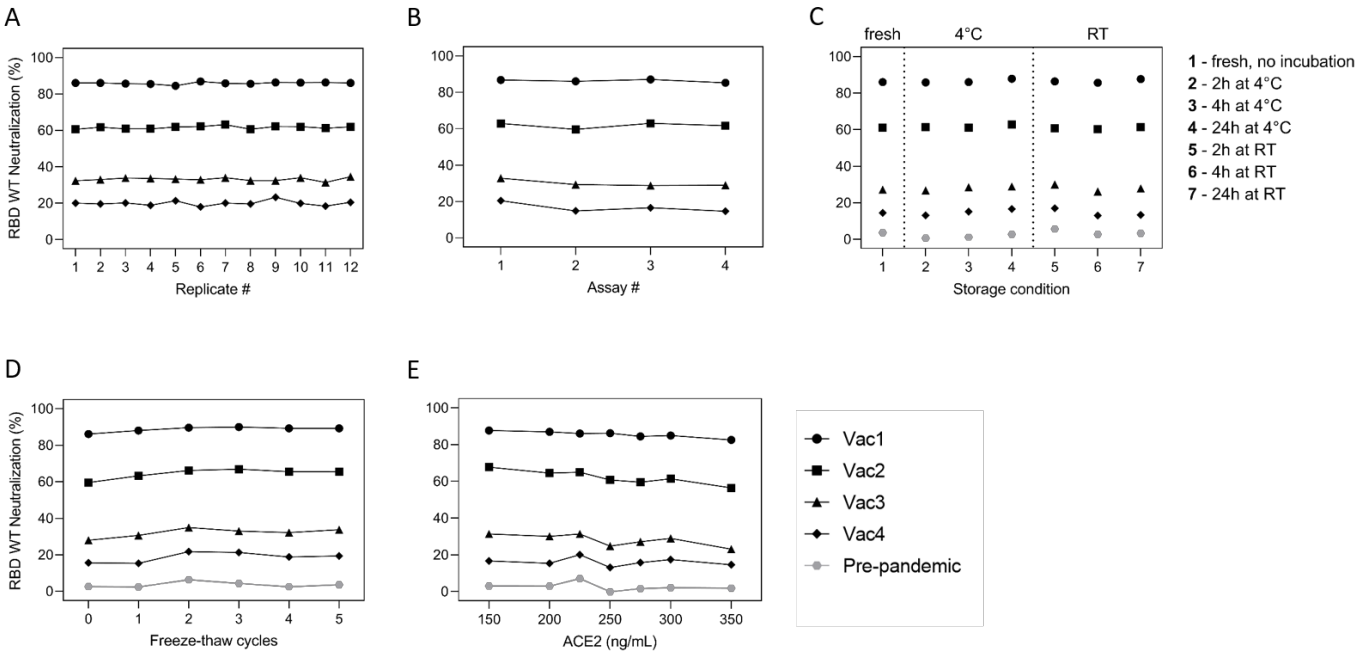

Figure 1 | ACE2 RBD competition assay: Technical validation results. Results of intra-assay precision **(A)**, inter-assay precision **(B)**, short-term stability **(C)**, freeze-thaw stability **(D)** and parallelism **(E)** experiments analyzing neutralization capacity (displayed as %) using wild-type (WT) RBD. Four samples from donors vaccinated with Pfizer BNT-162b2 (n=4, black) and one pre-pandemic sample (n=1, grey) were analyzed. Data points of each sample are illustrated by different shapes according to the figure key. Percent coefficients of variation (%CV) for all included RBD mutants are summarized in **Supplementary table 3**.

A

	ACE2 RBD Competition Assay (% Neutralization)		
NeutraLISA (% Inhibition)		≤ 20 %	> 20%
	≤ 20 %	59 (31.7 %)	6 (3.2 %)
	> 20 %	20 (10.8 %)	101 (54.3 %)
Pearson r [95% CI]	0.7954 [0.7357; 0.8428]		

B

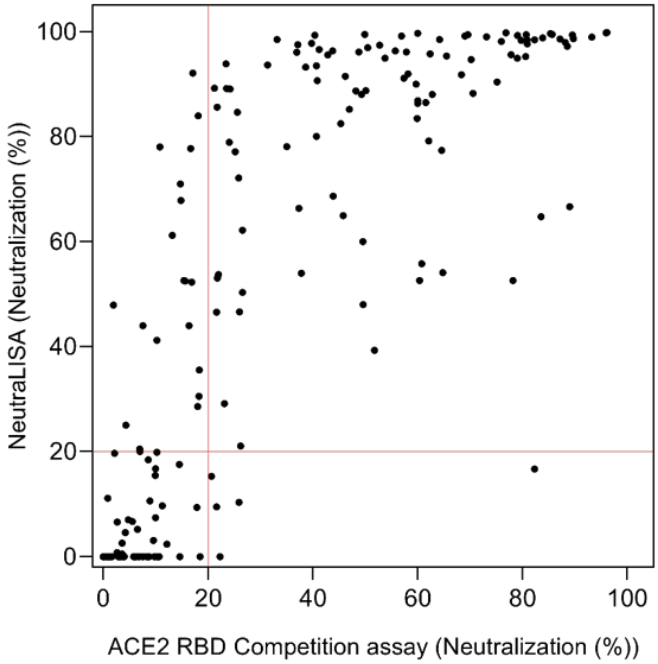

Figure 2 | Correlation between SARS-CoV-2 NeutraLISA and the multiplex ACE2 RBD competition assay. One sample from each individual (n=186) was measured using both assays and analyzed by linear regression. Samples were classified as being negative (non-neutralizing) if they had a value below 20% (red lines). **(A)** Descriptive statistics of the **(B)** linear regression, showing the distribution of samples as positive or negative for both assays. Correlation analysis was performed after Pearson and the correlation coefficient r is shown in the table with the 95 % confidence interval (CI).

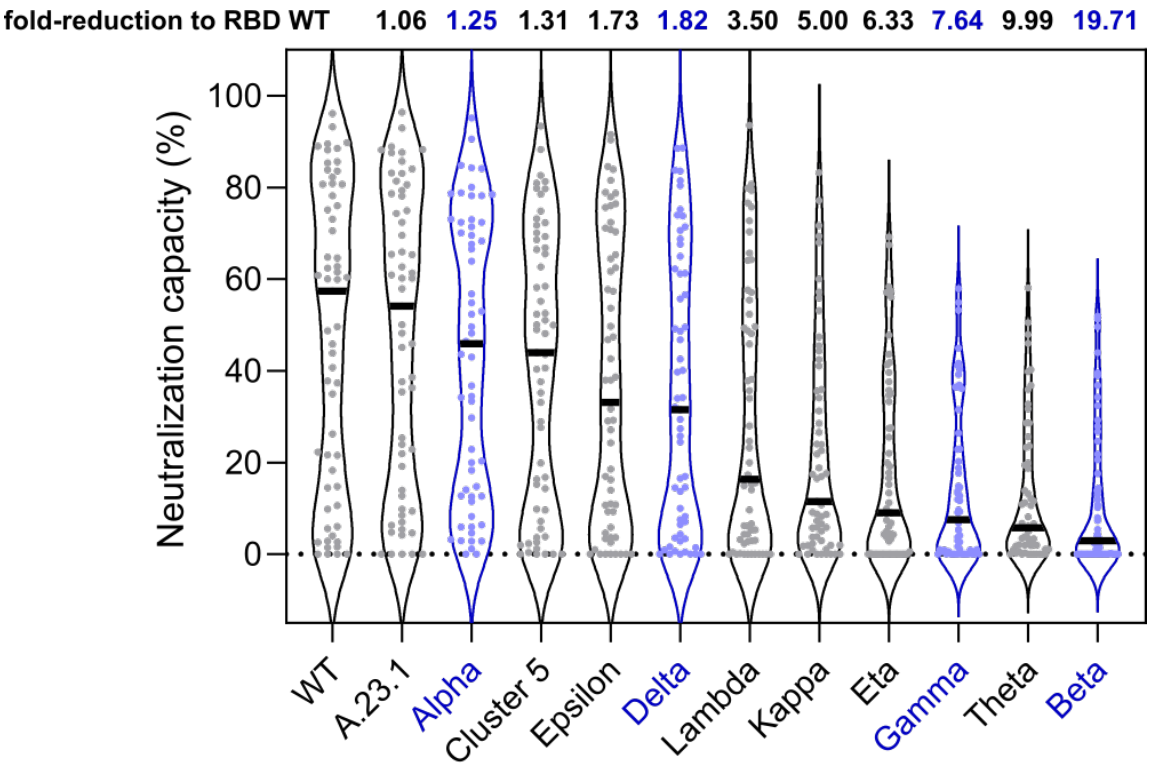

Figure 3 | Neutralization capacity varies between RBD mutants. Violin plots showing neutralization capacities (%) of individual serum samples from 7 to 49 days post PCR (n=59, depicted as dots) against RBD mutants. Black horizontal lines represent medians. Fold-decrease of neutralization capacity in comparison to wild-type corresponds to the ratio between the medians of wild-type and the respective RBD mutant. RBDs of VOC are shown in blue. An overview of the mutations present in all RBD mutants is shown in **Supplementary Table 1**.

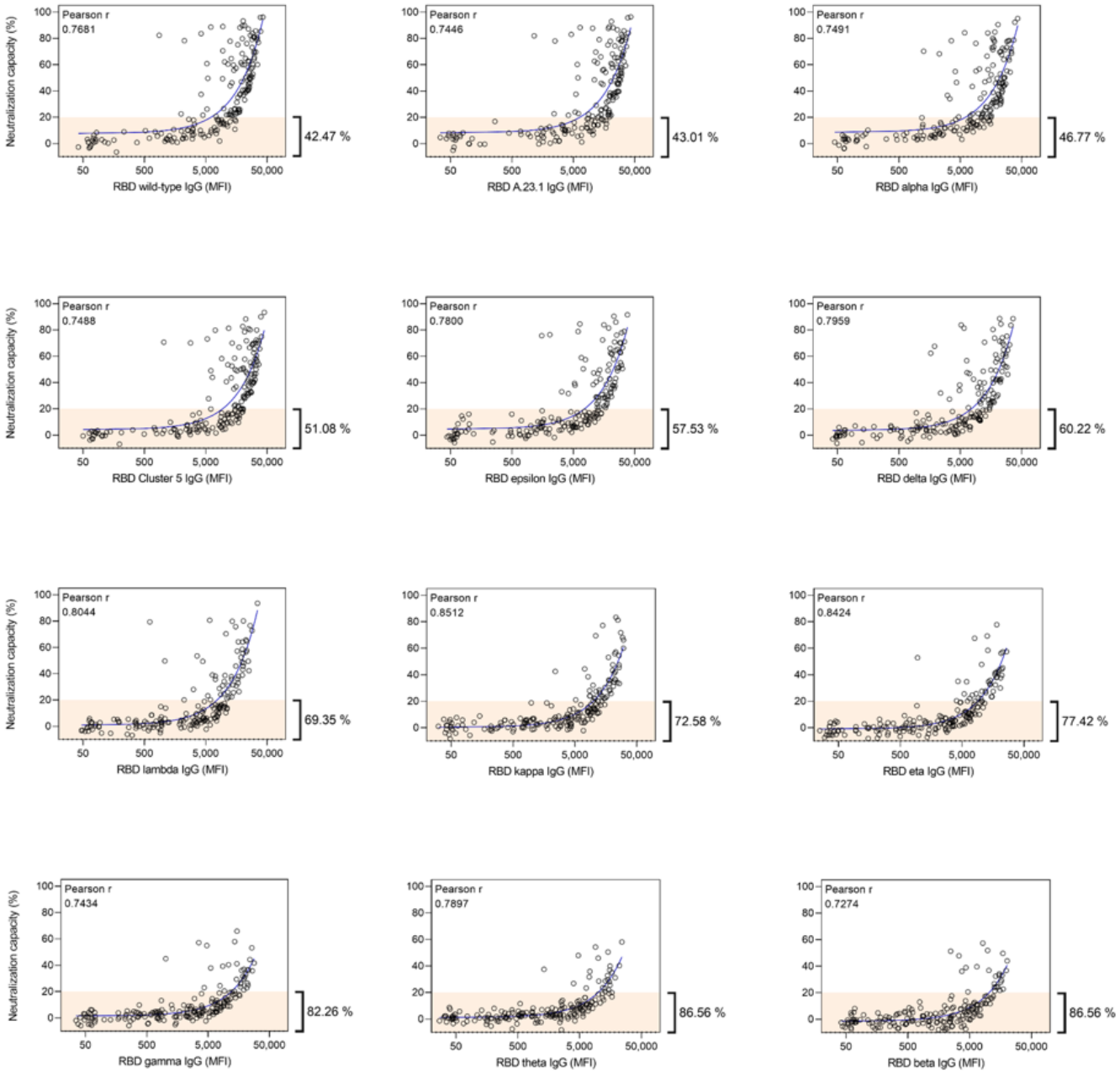

Figure 4 | Correlation between anti-RBD IgG MFI signals and neutralization capacities of serum samples from COVID-19 patients for wild-type and 11 RBD mutants. Regression analysis comparing neutralizing capacity (%) and IgG responses (MFI) for wild-type and all RBD mutants included in the study. Each circle represents one sample (n=186). For longitudinal donors with more than one sample available, the sample closest to 20 days post positive PCR diagnosis was selected. The percentage next to the bracket indicates the proportion of samples with neutralization capacity ≤ 20% (in orange). Pearson's correlation coefficient (r) is specified for every correlation.

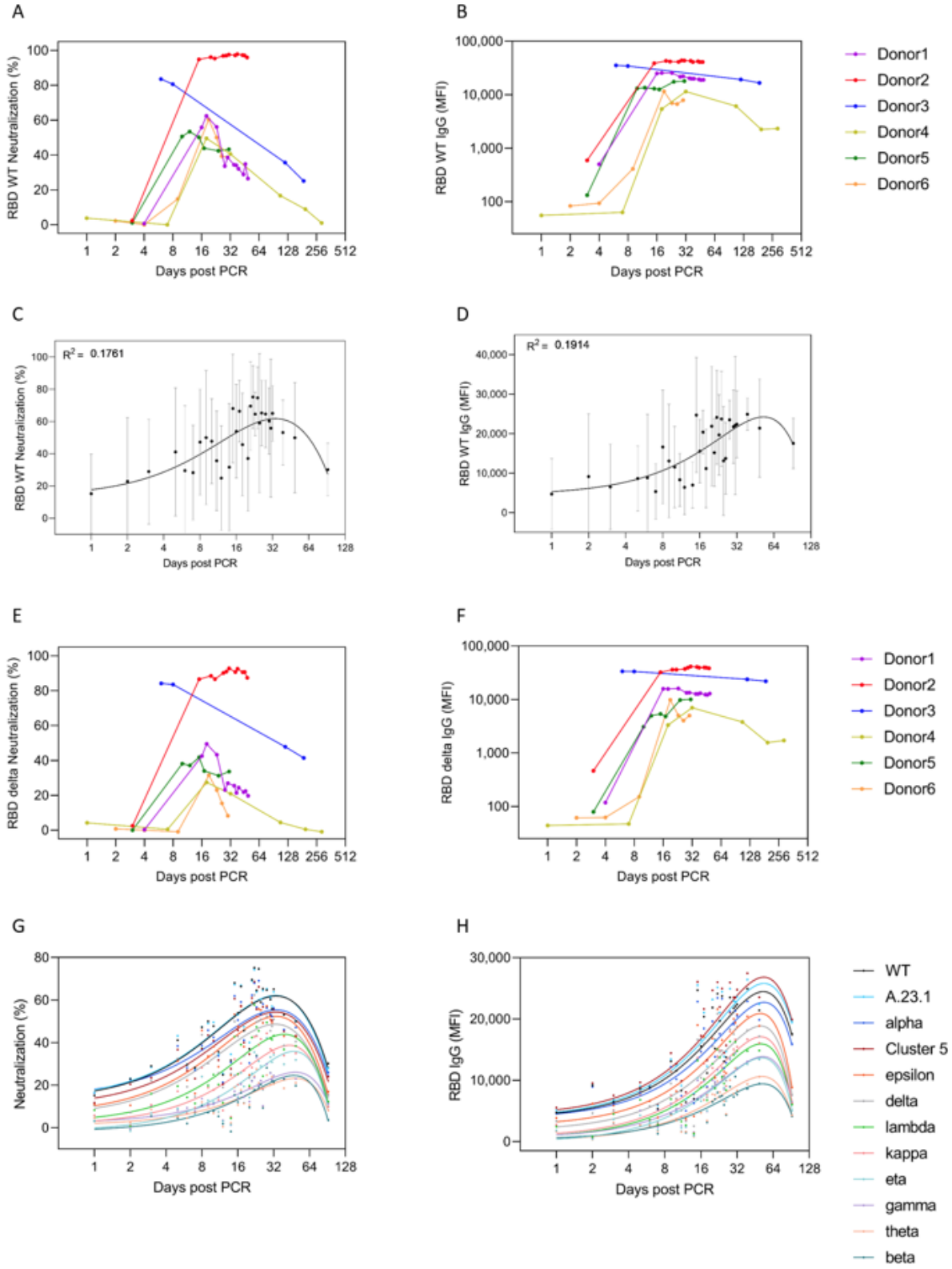

Figure 5 | Longitudinal analysis of anti-RBD IgG levels and neutralization capacities in Covid-19 patients. Neutralization capacity (%) and IgG responses (MFI) against time post positive PCR test for longitudinal samples of selected donors (n=6) for wild-type **(A, B)** and RBD delta **(E, F)**. The same analysis is then shown for all individual samples from 1 to 92 days post PCR (n=168) for wild-type **(C, D)**. Black dots indicate mean responses with standard deviation indicated by the error bars. Neutralization capacity (%) and IgG responses (MFI) 1 to 92 days post PCR for all RBD mutants included in the study **(G, H)**. Each variant is illustrated by a different color according to the figure key.

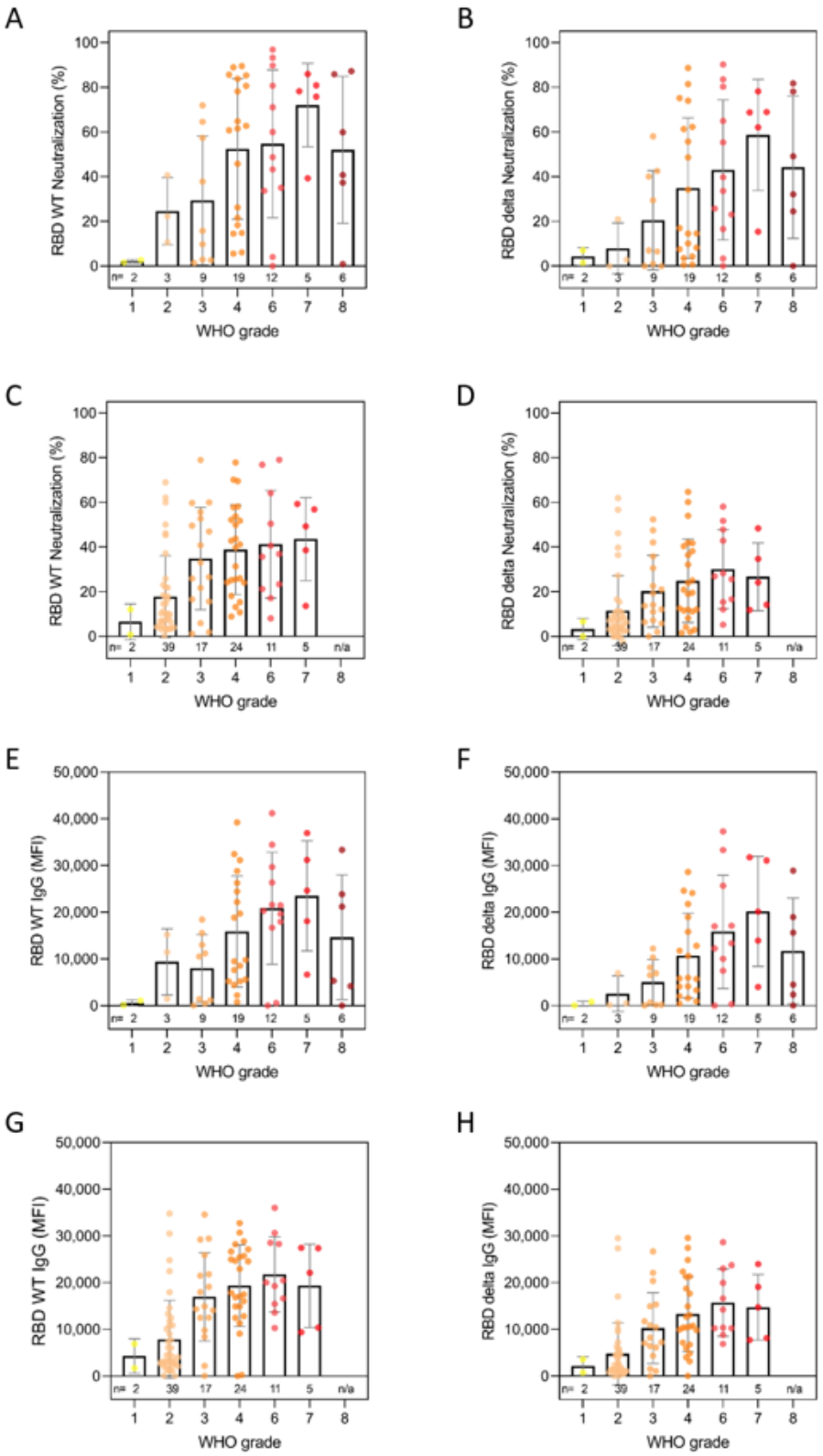

Figure 6 | Correlation of anti-RBD IgG levels and neutralization capacities with SARS-CoV-2 disease severity. Bar charts showing mean neutralization capacities (%) against wild-type and RBD delta are correlated with WHO grades for disease severity for samples 7-49 days post PCR **(A, B)** and later than 49 days post PCR **(C, D)**. Mean anti-RBD WT IgG and anti-RBD delta IgG levels are shown for samples 7-49 days post PCR **(E, F)** and later than 49 days post PCR **(G, H)**. Individual samples are displayed as colored dots, bars indicate the mean of the dataset with error bars representing standard deviation. Number of samples is given below the columns (n). If no samples for a group were available, the column is labeled with “n/a”. WHO grade 1 - ambulatory / no limitations of activities, 2 - ambulatory /

limitation of activities, 3 - hospitalized, mild disease / no oxygen therapy, 4 - hospitalized, mild disease / mask or nasal prongs, 6 - hospitalized, severe disease / intubation + mechanical ventilation, 7 - hospitalized, severe disease / ventilation + additional organ support (pressors, RRT, ECMO), 8 – Death. The study did not contain samples of WHO grade 5.

Supplementary Figures and Tables

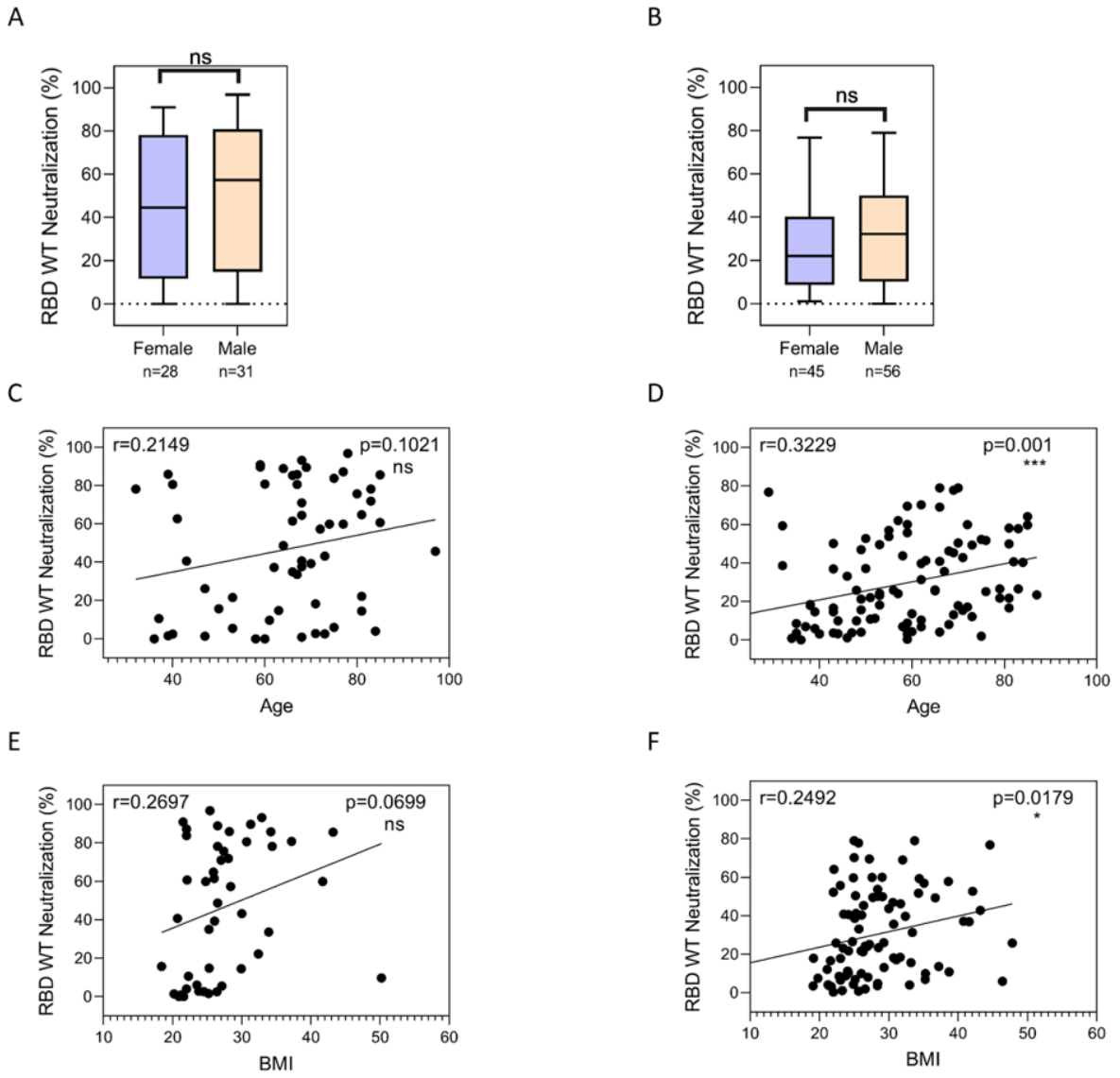

Supplementary Figure 1 | Relation between neutralization capacity and gender, donor age and Body-mass-index (BMI). Correlation between wild-type neutralization capacities (%) and gender (A, B), age (C, D) and BMI (E, F) for samples 7-49 days post PCR (A,C,E) and later than 49 days post PCR (B,D,F). P-values, when significant, are shown for all panels. Pearson's r was used to determine correlations.

Supplementary Table 1| Mutations of SARS-CoV-2 RBD proteins of 11 variants used in this study.

Variant	RBD mutations							
A.23.1	V367F							
Alpha								N501Y
Cluster 5				Y453F				
Epsilon			L452R					
Delta			L452R		T478K			
Lambda			L452Q			F490S		
Kappa			L452R				E484Q	
Eta							E484K	
Gamma		K417T					E484K	N501Y
Theta							E484K	N501Y
Beta		K417N					E484K	N501Y

Supplementary Table 2|Characteristics of the analyzed serum sample set.

Characteristic	
Number of donors	186
Number of samples	325
Median age (IQR) -years	62 (22)
Female sex (%)	84 (45.7)
Median ΔT post first positive PCR test (range)	85 (1-348)
Median BMI (range)	26.5 (18.4 – 50.2)

Supplementary Table 3 | ACE2 RBD competition assay validation results. Percentage coefficients of variation (%CV) of normalized MFI values for every bead region and RBD studied for every analyzed sample (n=5) and the mean of all samples.

	Samples	RBD WT	alpha	beta	gamma	epsilon	Cluster 5	A.23.1	eta	theta	kappa
Intra-assay precision (%CV)	Vac1	1.4	1.5	2.6	2.5	1.3	1.5	1.7	1.4	2.1	1.1
	Vac2	2.2	2.1	1.1	1.6	1.7	1.2	1.5	1.9	1.6	2.0
	Vac3	2.8	4.0	3.8	2.1	4.2	3.0	3.5	2.1	1.6	4.3
	Vac4	2.2	2.1	3.4	1.9	2.0	2.0	2.3	1.7	2.1	2.4
	Mean	**2.1**	**2.4**	**2.7**	**2.0**	**2.3**	**1.9**	**2.3**	**1.8**	**1.8**	**2.5**
Inter-assay precision (%CV)	Vac1	1.9	2.7	3.0	2.9	2.8	2.3	3.5	2.7	2.9	2.9
	Vac2	2.6	3.0	3.9	2.8	3.5	2.4	2.7	3.0	2.1	3.0
	Vac3	5.7	6.9	6.9	3.5	6.4	4.6	5.5	4.9	3.6	5.2
	Vac4	4.4	3.5	4.6	2.9	4.3	2.5	1.9	3.0	2.7	3.3
	Mean	**3.3**	**3.7**	**4.3**	**3.0**	**4.0**	**2.9**	**3.0**	**3.0**	**2.6**	**3.4**
Freeze-thaw stability (%CV)	Vac1	2.7	3.8	4.5	3.1	4.0	2.7	3.3	2.1	2.9	3.2
	Vac2	4.0	3.2	2.5	2.5	3.8	2.8	2.9	2.6	3.2	2.9
	Vac3	9.3	10.2	4.7	5.8	12.1	8.9	7.3	9.8	5.5	10.6
	Vac4	7.6	6.2	6.1	5.3	7.2	5.8	6.6	6.3	4.9	6.3
	Pre-pandemic	1.8	1.8	3.2	3.7	1.8	1.4	2.1	2.3	2.3	2.0
	Mean	**4.8**	**4.7**	**4.2**	**3.9**	**5.3**	**4.1**	**4.1**	**4.3**	**3.5**	**4.7**
Short-term stability (%CV)	Vac1	2.5	3.9	3.2	2.3	2.5	2.3	2.6	2.1	2.8	3.2
	Vac2	2.3	3.1	4.5	2.3	2.3	2.8	2.6	2.0	2.4	2.6
	Vac3	8.6	9.3	6.4	3.0	6.9	4.4	4.9	7.1	3.2	7.3
	Vac4	11.6	4.9	3.4	3.2	3.0	2.4	3.1	3.2	2.3	3.3
	Pre-pandemic	1.6	2.3	3.7	1.9	1.9	1.8	2.2	1.8	2.4	2.1
	Mean	**4.8**	**4.7**	**4.2**	**3.9**	**5.3**	**4.1**	**4.1**	**4.3**	**3.5**	**4.7**
Parallelism (%CV)	Vac1	4.1	3.9	5.0	4.0	4.5	4.2	4.2	3.2	2.6	3.9
	Vac2	4.2	2.5	4.0	3.4	2.7	2.5	4.2	2.6	2.8	4.2
	Vac3	12.0	11.7	4.0	5.3	11.9	11.8	9.3	13.6	4.5	12.7
	Vac4	11.3	9.6	6.5	6.9	10.0	8.7	8.6	9.9	4.4	9.3
	Pre-pandemic	2.1	1.2	3.6	2.8	2.3	2.1	2.4	1.9	2.7	1.4
	Mean	**4.8**	**4.7**	**4.2**	**3.9**	**5.3**	**4.1**	**4.1**	**4.3**	**3.5**	**4.7**